PROCEEDINGS.Twenty-Second Workshop on Geothermal Reservoir Engineenng
Stanford University, Stanford.California, January 27-29, 1997
SGP-TR-155

FRACTURE PERMEABILITY AND ITS RELATIONSHIP TO IN-SITU STRESS IN THE DIXIE VALLEY, NEVADA, GEOTHERMAL RESERVOIR

Colleen A Barton[1], Stephen Hickman?, Roger Morin[3],
Mark D. Zoback', Thomas Finkbeiner', John Sass[4] and Dick Benoit[5]

'Stanford University, Dept. of Geophysics, Stanford, CA 94305, USA
barton@pangea.stanford.edu,zoback@pangea.stanford.edu,fink@pangea.stanford.edu
[2]U.S. Geological Survey, Menlo Park, CA 94025, USA
hickman@thepub.wr.usgs.gov
'U.S. Geological Survey, Denver, CO 80225, USA
rhmorin@borehole.cr.usgs.gov
[4]U.S. Geological Survey, Flagstaff, AZ 86001, USA
jsass@flagmail.wr.usgs.gov
[5]Oxbow Geothermal Corp., Reno, NV 89502, USA
dick_benoit@opsi.oxbow.com

ABSTRACT

An extensive suite of spinner flowmeter, high-resolution temperature and borehole televiewer logs were acquired in a 2.7-km-deep well drilled into a fault-hosted geothermal reservoir at Dixie Valley, Nevada. Localized perturbations to wellbore temperature and flow were used to identify hydraulically conductive fractures. Comparison of these data with fracture orientations from the borehole televiewer logs indicates that hydraulically conductive fractures in crystalline rocks within and adjacent to the producing fault zone have an orientation distinct from the overall fracture population. In conjunction with in-situ stress measurements from this well [Hickman et al., this volume]. Coulomb analysis indicates that these permeable fractures are critically stressed, potentially active normal faults in the current west-northwest extensional stress regime at Dixie Valley.

INTRODUCTION

It is generally accepted that fractures control hydrologic properties in crystalline rocks. Therefore, understanding fluid flow in the fractured, low-porosity rocks comprising the Dixie Valley geothermal reservoir requires detailed knowledge of fracture and fault orientations and their hydraulic properties as well as the in-situ state of stress.

In situ measurements indicate that in many regions of active deformation, the state of stress is controlled by the frictional strength of optimally oriented faults. In such areas, the magnitude and orientation of the principal stresses are in accordance with simple Coulomb faulting theory, laboratory-derived coefficients of friction and in situ pore pressure. In several boreholes in the western U.S. where detailed information is available on in situ stress, fracture and fault orientation and relative fracture permeability, it has been demonstrated that the fractures controlling bulk permeability are optimally oriented shear faults [Barton, Zoback and Moos, 1995].

Fractures and faults are introduced into a rock mass throughout its history, and consequently, may not bear a simple relationship to the contemporary stress field [Seeburger and Zoback, 1982; Segall, 1990; Barton and Zoback, 19921. However, the current stress field can control which fractures and faults will affect properties such as fluid flow. Thus, to understand the fluid flow regime where it is dominated by fault and fracture permeability, it is necessary both to determine the distribution and orientation of the fractures and faults and to relate them to the present-day stress field.

In this study we use data from a 3-km-deep borehole penetrating a geothermal reservoir associated with an active normal fault at Dixie Valley, Nevada, to better understand the relationship between fracture and fault permeability and the contemporary in situ stress field. The results from in-situ stress measurements in this

well are presented by Hickman and Zoback (this volume).

The Dixie Valley Geothermal Field is located within the western Basin and Range in west central Nevada in an area of recent seismicity, high heat flow and late Cenozoic volcanic activity [Thompson and Burke, 1973; Bruhn, et al., 19941. Dixie Valley is flanked by the Stillwater Range to the West and the Clan Alpine and Augusta Mountains to the east. Upper crustal extension in this region has faulted, tilted and fractured diverse Mesozoic and Paleozoic sedimentary and igneous rocks as well as massive Tertiary basalt flows. Dixie Valley is a structurally asymmetric basin bounded by a single zone of faulting on the northwest and by step faulting to the southeast [Okaya and Thompson, 19851. The Stillwater Fault to the northwest dips 52°-54° and is planar to a depth of 3 km. This fault zone is marked by a band of hydrothermal alteration and fracturing a few meters to several hundred meters wide that extends for 10's of km in the footwall adjacent to Quaternary scarps.

The regional hydrology of Dixie Valley constitutes a closed hydrologic unit covering 5182 **sq.** km of surface drainage [Parchman and Knox, 1981]. Movement of water from ephemeral streams, springs, and winter snow melt occurs as subsurface flow through Cenezoic sediments. Groundwater recharge occurs by infiltration of meteoric water through faults and fractures within the consolidated rocks of the mountain ranges with movement towards the valley occurring as groundwater underflow. As the water descends it is heated by the regional temperature gradients and begins to convect upward. Hot water moving up along the Stillwater range faults causes abnormally high temperature gradients to penetrate the basin fill material. These high temperature gradients appear to be fault controlled and are confined to a narrow, elongated wedge along the front of the Stillwater range. Temperature gradients along this zone have been mapped at 100°C/km and reach 200°C/km at some locations [see Williams, et al., this volume].

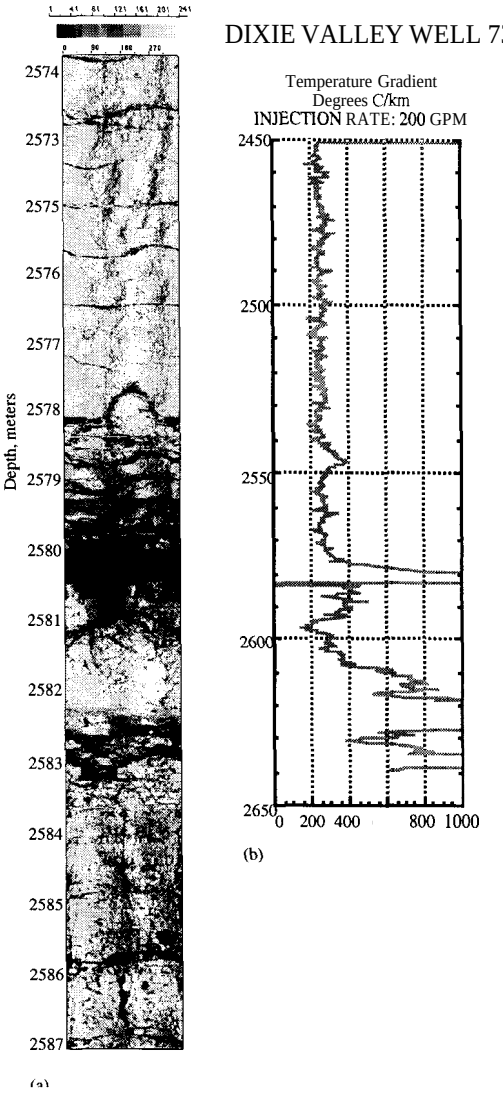

Fig. 1.(a) High Temperature Borehole televiewer data recorded over the interval 2574 - 2587 m in well 73B-7 and (b) precision temperature **data** recorded over the interval 2450 - 2650 m in this well. The images in Figure l a are oriented with respect to true North (right and left margins).

DATA ACQUISITION AND ANALYSIS

An extensive open-hole logging program was conducted in the 73B-7 borehole at Dixie Valley from September to November, 1995, during which we obtained approximately 2 km of borehole televiewer (BHTV) logs together with precision temperature and spinner flowmeter logs (see Figure 1). Excellent quality televiewer images were recorded and have been digitally processed for fracture distribution and geometry. Using these logs, we have located and oriented faults, fractures and drilling induced fractures (e.g., thermal tensile fractures). The Stanford and USGS high-temperature borehole televiewers were used to log this well. Fundamentals of the operation of these acoustic tools are described in detail in Zemanek [19701. The strike, dip and apparent aperture of the fractures has been measured using the digital BHTV analysis system developed at Stanford University [see Barton et al., 19911.

To date, we have digitized and analyzed approximately 1850 meters of analog borehole televiewer (BHTV) data recorded in well 73B-7. After the data were calibrated they were processed and edited for systematic noise and other tool related problems. An example of the BHTV data obtained in this well is shown in Figure 1a, where several natural fractures (represented as sinusoids) cross-cut the borehole.

The orientations of all fractures within the fault zone interval are shown in lower hemisphere stereographic projection of poles to fracture planes and contoured poles to fracture planes (Figure 2a and 2b, respectively). The overall fracture population in this well has significant scatter in orientation but fractures generally become steeper and larger in apparent aperture with depth. The dominant fracture strike ranges from north to east with shallow to moderate dips to the southeast. The local orientation of the Stillwater fault is shown for reference as the large gray dot in Figure 2b.

Precision temperature and spinner flowmeter logs were acquired in borehole 73B-7 at Dixie Valley, with and without simultaneously injecting water into the well. Fluid flow into or out of individual fractures and faults was determined through an analyses of these temperature and spinner flowmeter logs [see Paillet and Ollila, 19941. When a borehole is close to thermal equilibrium with the surrounding rock, heat transfer occurs primarily by thermal conduction and the temperature gradient in the borehole is a function of thermal conductivity and heat flux. Localized perturbations to well-bore temperature will result from localized fluid flow into or out of the borehole and can be detected by precision temperature logging. Fractures or faults that correlate in depth with these

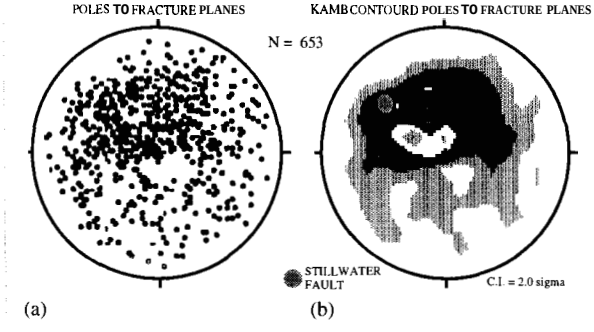

Fig. 2. (a) Lower hemisphere, equal area projections of poles to all fracture planes and (b) Kamb contoured poles to planes measured over the interval 1850 - 2640 m in well 73B-7 at Dixie Valley [after Kamb, 1959].

localized temperature perturbations are therefore considered to be hydraulically conductive. Multi-pass temperature logs at various pumping rates allow us to assess the persistence of these detected flow horizons.

Flow logs recorded at different injection rates were also analyzed to obtain quantitative measures of permeability over discrete intervals in well 73B-7. We evaluated spinner flowmeter logs, under static and injecting conditions, to determine the relative rates of fluid inflow or outflow over discrete intervals in the well and to measure permeabilities over these intervals. Flowmeter logs conducted at different injection rates have isolated two intervals of the Stillwater Fault Zone penetrated by well 73B-7 as the primary fluid producing zones. Both zones have relatively high bulk permeabilities. The upper zone from 2613 to 2615 m has a permeability of approximately 2.1×10^{-11} m^2 (21 Darcies) and the lower zone between 2626 and 2628 m has a permeability of 4.8×10^{-11} m^2 (48 Darcies).

HYDRAULICALLY CONDUCTIVE FRACTURES WITHIN THE STILLWATER FAULT ZONE

As described above, we have used the BHTV data in conjunction with precision temperature logs and spinner flowmeter logs to differentiate between permeable fractures and the large number of natural fractures penetrated by the borehole. With the stress state determined [Hickman and Zoback, this volume], we were able to relate stress orientations and magnitudes, fluid flow indicators and bulk reservoir hydrologic properties to the orientations and relative apertures of fractures and faults.

An example of the type of temperature data used in this study is presented in Figure 1b where a very large fracture at 2588 m is clearly perturbing the temperature gradient at this depth (Figure 1b). In addition, several fine scale temperature gradient anomalies are apparent in Figure 1b which correlate with distinct fractures in the image data.

Temperature logs commonly contain some degree of noise due to the extremely high sensitivity of the probe. To eliminate the exaggeration of this noise in the temperature gradient profiles a 1.5 m depth smoothing was applied to the temperature data before computing the temperature gradient.

Non-equilibrium thermal conditions in Well 73B-7 during logging resulted in a non-uniform temperature

gradient. To account for this effect and to minimize subjectivity, temperature anomalies were selected by establishing a temperature gradient cutoff value that vaned with depth, above which the largest anomalies were distinct. The background temperature gradient at each depth was calculated using a moving window of 5 meters. Anomalies in the temperature gradient profile of ±50°C/km above this average temperature gradient were used to identify permeable features.

Fractures detected using borehole image data within ±1.0 m of an isolated temperature anomaly were assumed responsible for fluid flow at the anomaly. If more than one fracture was present within ±1.0 m of the temperature anomaly, the dominant fracture orientation was selected. A subset of hydraulically conductive fractures was selected from the total fracture population using this technique.

A control population of non-hydraulically conductive fractures was also be extracted from the total fracture population. For each 1 meter interval with no indication of fluid flow (no temperature gradient anomaly above the designated cutoff value) a fracture was selected that again represented the dominant fracture trend for that 1 meter interval.

Lower hemisphere equal area stereographic projections of poles to both hydraulically-conductive and non-hydraulically conductive fractures indicate that the conductive fractures observed in this well are a distinct subset of the entire fracture population (Figure 3).

From the analysis of both the spinner flowmeter and temperature log data only six fractures appear to dominate fluid flow within well 73B-7. These

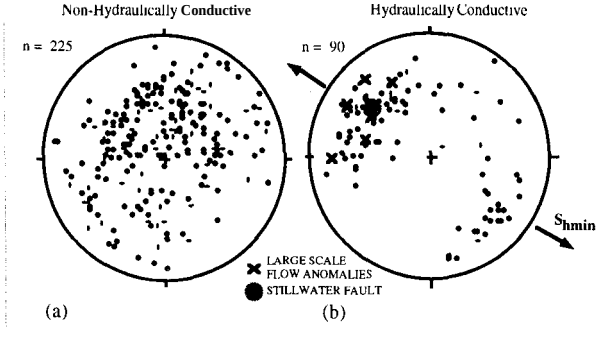

Fig. 3. Poles to non-hydraulically conductive fractures and (b) poles to hydraulically conductive fractures. The local orientation of S_{hmin} is from Hickman and Zoback [this issue].

fractures, associated both with large perturbations in temperature and large changes in flowrate, are shown as the "x" symbol in Figure 3b.

We used the Coloumb failure criterion [see Jaeger and Cook, 19791 to determine whether each of the hydraulically and non hydraulically conductive fractures observed in well 73B-7 was a potentially active fault. If one assumes that these fractures have zero cohesion and using laboratory friction values reported by Byerlee [1978], this criterion predicts that planes with a ratio of shear stress to effective normal stress (i.e., normal stress minus pore pressure) ≥ 0.6 are critically stressed for frictional failure.

The shear and normal stresses acting on each fracture plane are a function of the principal stress magnitudes and the orientation of the fracture plane with respect to the orientation of the principal stresses. Hickman and Zoback [this volume; their Figure 3] present the stress magnitudes and pore pressures we used to compute shear and effective normal stresses on the permeable and impermeable fracture planes in well 73B-7. For the sake of simplicity, we have used linear approximations to the values reported by Hickman and Zoback. The values that we used for the vertical gradients in the vertical stress, S_v, range from 22.9 MPa/km in the sediments above 2150 m to 26.7 MPa/km in the primarily crystalline rocks below this depth. We also assumed that the formation fluid pressure increases linearly from zero starting at a depth of 152 m at the rate of 9.0 MPa/km. The least principal stress, S_{hmin}, magnitudes measured by Hickman and Zoback in well 73B-7 and the nearby shallow well 24W-5 were approximated in our analysis using a gradient of 12.5 MPa/km, with a zero-depth intercept of -2.0 MPa. We used a value of 18.5 MPa/km for the vertical gradient of the maximum horizontal principal stress, S_{Hmax}, with a zero depth intercept of -6.5 MPa, which is intermediate between the S_{hmin} and S_v stress gradients. The azimuth of S_{Hmax} used in this analysis is 33°, based upon observations of wellbore failure in this well by Hickman and Zoback.

The results of this analysis are shown as 3D Mohr diagrams in Figure 4. Since a large percentage of the hydraulically conductive fractures lie between the Coloumb failure lines for μ=0.6 and μ=1.0 (Figure 4a), these features appear to be critically stressed, potentially active faults in frictional equilibrium with the current in-situ stress field at Dixie Valley. Note that the majority of fractures not associated with temperature anomalies clearly lie below the Coloumb

failure curve for μ=0.6 and, therefore, do not appear to be critically stressed shear fractures (Figure 4b).

As discussed by Hickman and Zoback [this volume] the magnitude of S_{Hmax} in well 73B-7 is less well-constrained than are the other stress magnitudes. Their breakout analysis indicates that the magnitude of S_{Hmax} lies somewhere between S_v and S_{hmin}. For this study we utilize a stress gradient for S_{Hmax} that is midway between S_v and S_{hmin}. Analyzing the propensity for frictional failure over the full range $S_{hmin} \leq S_{Hmax} \leq S_v$, however, shows that most of the permeable fractures still appear to be critically stressed failure planes, regardless of the S_{Hmax} magnitudes used.

CONCLUSIONS

We have measured the distribution and orientation of faults and fractures within geothermal reservoir rocks penetrated by Dixie Valley Well 73B-7 and studied their hydrologic properties through comparison with fracture-related thermal and flow anomalies. By documenting systematic relationships between fracture orientation and hydrologic properties (e.g., permeability) and the in-situ state of stress, we hope to provide a conceptual framework for interpreting the hydrology of reservoir rocks in the Dixie Valley geothermal field.

The results of this analysis indicate that hydraulically conductive fractures have an orientation that is distinct from the overall orientation of fractures and faults within and adjacent to the Stillwater Fault Zone. Comparison of these fracture orientations with in-situ stress data obtained in this well by Hickman and Zoback [this volume] indicates that these hydraulically conductive fractures are optimally oriented for frictional failure in the northwest-southeast extensional stress regime at Dixie Valley.

Oxbow Geothermal has made available additional wells drilled within the geothermal reservoir at the Dixie Valley site for flow tests, borehole imaging and hydraulic fracturing tests. These wells will provide additional constraints on the stress field when analyzed in conjunction with results obtained from this study. Further, three of these wells are not sufficiently permeable to be of commercial value. Data from wellbore imaging, stress measurements and flow tests in these wells will help determine if there are variations in fracture orientation, in-situ stress regime, or other factors that might explain the observed variations in permeability along the Stillwater fault zone.

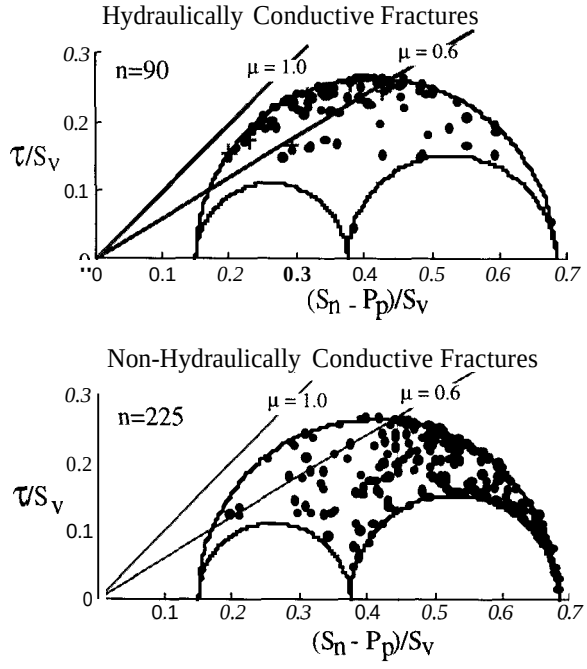

Fig. 4. Normalized shear stress versus effective normal stress for (a) hydraulically conductive and (b) non-hydraulically conductive fractures in well 73B-7, based on precision temperature logs (refer to Jaeger and Cook, 1979, p.28, for details on construction of these diagrams). The large gray circle represents the shear and normal stress for the Stillwater Fault zone in the vicinity of the well. Gray "+" symbols represent fractures primarily responsible for fluid flow in Well 73B-7, within and adjacent to the Stillwater fault zone.

REFERENCES

Barton, **C.A.,** M.D. Zoback and D. Moos. Fluid flow along potentially active faults in crystalline rock, *Geology*, **23,** 8, 683-686 (1995).

Barton, C. **A.,** L. Tesler, and M. D. Zoback, Interactive analysis of borehole televiewer data, in *Automated pattern analysis in petroleum exploration,* edited by I. Palaz and S. Sengupta, pp. 217-242, Springer-Verlag (1991).

Barton, **C.** A., and **M.** D. Zoback, Self-similar distribution and properties of macroscopic fractures at

depth in crystalline rock in the Cajon Pass scientific drill hole, *J. of Geophys. Res.,* **97,** 5181-5200 (1992).

Bruhn, R. L., W.T. Parry, W. A. Yonkee, T. Thompson, Fracturing and hydrothermal alteration in normal fault zones; PAGEOPH, 142, 3/4, 609-644 (1994).

Byerlee, J. Friction of rocks: ***PAGEOPH,*** **116,** 615-626 (1978).

Jaeger, J.C. and Cook, N. G. W., Fundamentals of Rock Mechanics (third Edition): New York, Chapman and Hall, p.28-30, 1979.

Kamb, W.B., Ice petrofahric observations from Blue Glacier, Washington, in relation to theory and experiment, J. Geophys. Res., **64,** 1891-1910, (1959).

Okaya, D.A., and G. A. Thompson, Geometry of Cenozoic extensional faulting, Dixie Valley, Nevada, *Tectonics,* **4,** 107-125, (1985).

Paillet, F. L., and P. Ollila, Identification, characterization, and analysis of hydraulically conductive fractures in granitic basement rocks, Millville, Massachusetts , *Water Resources Investigations, U.S.G.S.,* WRI 94-4185, (1994).

Parchman, W.L. and J.W. Knox, Exploration for geothermal resources in Dixie Valley, Nevada, *G.R.C. Bull.,* **10,** 5, 3-6, (1981).

Seeburger, D. **A., and** M. D. Zoback, The distribution of natural fractures and joints at depth in crystalline rock, ***J. Geophys. Res.,*** ***87,*** 5517-5534, (1982).

Segall, P., Late Cretaceous age of fractures in the Sierra Nevada Batholith, California, *Geology,* **18,** 1248-1251, (1990).

Thompson G. A. and Burke D.B. Regional geophysics of the Basin and Range province, Nevada, *Geol. Soc. Am. Bull.,* 84, 627-632, (1973).

Zemanek, J., E. E. Glenn, L. J. Norton, and R. L. Caldwell, Formation evaluation by inspection with the borehole televiewer, *Geophysics,* **35,** 254-269, (1970).